

The weak-line T Tauri star V410 Tau

I. A multi-wavelength study of variability

B. Stelzer¹, M. Fernández², V. M. Costa^{3,4}, J. F. Gameiro^{3,5}, K. Grankin⁶, A. Henden⁷, E. Guenther⁸, S. Mohanty⁹,
E. Flaccomio¹, V. Burwitz¹⁰, R. Jayawardhana¹¹, P. Predehl¹⁰, and R. H. Durisen¹²

¹ Osservatorio Astronomico di Palermo, Piazza del Parlamento 1, I-90134 Palermo, Italy

² Instituto de Astrofísica de Andalucía, CSIC, Camino Bajo de Huétor 24, E-18008 Granada, Spain

³ Centre for Astrophysics, University of Porto, Rua das Estrelas, 4150 Porto, Portugal

⁴ Departamento de Matemática, Instituto Superior de Engenharia do Porto, 4150 Porto, Portugal

⁵ Departamento de Matemática Aplicada, Faculdade de Ciências da Universidade do Porto, 4169 Porto, Portugal

⁶ Ulug Beg Astronomical Institute, Astronomicheskaya 33, 700052 Tashkent, Uzbekistan

⁷ USRA/USNO Flagstaff Station, P. O. Box 1149, Flagstaff, AZ 86002-1149, USA

⁸ Thüringer Landessternwarte, Karl-Schwarzschild-Observatorium, Sternwarte 5, D-07778 Tautenburg, Germany

⁹ Harvard-Smithsonian Center for Astrophysics, 60 Garden Street, Cambridge, MA 02138, USA

¹⁰ Max-Planck Institut für extraterrestrische Physik, Postfach 1312, D-85741 Garching, Germany

¹¹ University of Michigan, 953 Dennison Building, Ann Arbor, MI 48109, USA

¹² Indiana University, 727 E. 3rd Street, Bloomington, IN 47405-7105, USA

Received <16-06-2003> / Accepted <04-09-2003>

Abstract. We present the results of an intensive coordinated monitoring campaign in the optical and X-ray wavelength ranges of the low-mass, pre-main sequence star V410 Tau carried out in November 2001. The aim of this project was to study the relation between various indicators for magnetic activity that probe different emitting regions and would allow us to obtain clues on the interplay of the different atmospheric layers: optical photometric star spot (rotation) cycle, chromospheric H α emission, and coronal X-rays. Our optical photometric monitoring has allowed us to measure the time of the minimum of the lightcurve with high precision. Joining the result with previous data we provide a new estimate for the dominant periodicity of V410 Tau (1.871970 ± 0.000010 d). This updated value removes systematic offsets of the time of minimum observed in data taken over the last decade. The recurrence of the minimum in the optical lightcurve over such a long timescale emphasizes the extraordinary stability of the largest spot. This is confirmed by radial velocity measurements: data from 1993 and 2001 fit almost exactly onto each other when folded with the new period. The combination of the new data from November 2001 with published measurements taken during the last decade allows us to examine long-term changes in the mean light level of the photometry of V410 Tau. A variation on the timescale of 5.4 yr is suggested. Assuming that this behavior is truly cyclic V410 Tau is the first pre-main sequence star on which an activity cycle is detected. Two X-ray pointings were carried out with the *Chandra* satellite simultaneously with the optical observations, and centered near the maximum and minimum levels of the optical lightcurve. A relation of their different count levels to the rotation period of the dominating spot is not confirmed by a third *Chandra* observation carried out some months later, during another minimum of the 1.87 d cycle. Similarly we find no indications for a correlation of the H α emission with the spots' rotational phase. The lack of detected rotational modulation in two important activity diagnostics seems to argue against a direct association of chromospheric and coronal emission with the spot distribution.

Key words. stars: individual: V410 Tau – stars: late-type, coroneae, activity – X-rays: stars

1. Introduction

V410 Tau is an analog for the young Sun on the pre-main sequence (PMS). Due to the lack of strong emission lines and infrared excess it can be classified as a weak-line T Tauri star (wTTS). This term defines PMS stars without obvious signs for disk accretion, while young stars, in which accre-

tion from a circumstellar disk is responsible for ultraviolet and infrared excess emission and for a moderate to strong emission line spectrum superimposed on the photospheric spectrum, are called classical T Tauri stars (cTTS). Indeed, V410 Tau shows a small infrared excess which, however, is attributed to one or two close companions at sub-arcsecond separation (Ghez et al. 1993; Ghez et al. 1997).

WTTS represent an evolutionary stage where the disk has already dissipated, and therefore their variability is not re-

Send offprint requests to: B. Stelzer

Correspondence to: stelzer@astropa.unipa.it

lated to accretion processes but believed to be a manifestation of magnetic activity, similar to that observed in the Sun, but enhanced by several orders of magnitudes. Magnetic activity seems to explain all the optical variability phenomena discovered on V410 Tau, comprising a large range of time scales: *i*) variability of the amplitude of the optical light curve on time scales of years; *ii*) changes in the $H\alpha$ profile and intensity recorded within months; *iii*) repeated modulation of the optical brightness with a period of 1.87 d; and *iv*) sudden brightenings and/or emission line enhancements evolving on time scales of hours.

Items *i*) and *iii*) point directly at the presence of star spots. The periodic 1.87 d variability of the optical lightcurve of V410 Tau was first reported by Rydgren & Vrba (1983), and confirmed by subsequent observations (Vrba et al. 1988; Bouvier & Bertout 1989). It is attributed to stellar spots which produce a periodic rotation pattern. From these studies it is shown that about 15 – 45 % of the stellar surface of V410 Tau should be covered by spots in order to explain the large amplitudes observed in the optical bands. The models indicated temperatures for the spot(s) that are 500 K to 1200 K cooler than the photosphere, similar to the solar case (Wallace et al. 1996). Independent evidence confirming the spot hypothesis was provided by high-resolution spectroscopic observations: large ($\geq 10\%$) fractions of the stellar surface at about 1000 K below the photospheric temperature can considerably alter the profile of photospheric lines (Vogt & Penrod 1983, Vogt et al. 1987). The first Doppler images of V410 Tau were published by Joncour et al. (1994) and Strassmeier et al. (1994), and were confirmed by Hatzes (1995) and Rice & Strassmeier (1996). All of them show a large cool spot that extends over one of the stellar poles and smaller cool features located at low latitudes.

Longterm variability of the photometric amplitude could be related to changes in the number, size and location of spots. Longterm periodic changes in photometric lightcurves of a number of solar-analogs (Messina & Guinan 2002, Berdyugina et al. 2002) and more evolved RS CVn binaries (e.g. Henry et al. 1995, Rodonó et al. 2000, Olah et al. 2000) have been interpreted as magnetic activity cycles. Among younger PMS stars a lack of dedicated monitoring programs has long impeded any systematic investigation of this issue. First results on longterm photometry including PMS stars were reported by Strassmeier et al. (1997) based on observations at automated photoelectric telescopes. Thanks to the efforts of Vrba et al. (1988), Herbst (1989), Petrov et al. (1994), Strassmeier et al. (1997), and Grankin (1999) V410 Tau has by far the largest data base of photometry among the PMS stars. Although smooth changes in the amplitude of the optical light curve have been reported, no cyclic or predictable behavior has been found yet.

The origin of variations in emission lines [items *ii*) and *iv*) of the above list] is sometimes less obvious. $H\alpha$ observations of V410 Tau reveal slow changes both in the emission line profile and its intensity. There are two kinds of changes: smooth variations of the line profile and intensity within weeks (e.g. Petrov et al. 1994), that sometimes correlate with the photometric 1.87 d period (Fernández & Miranda 1998) and other, stronger, variations that are noticed when com-

paring data taken months apart from each other (previous references; Hatzes 1995). Petrov et al. (1994) suggest a chromospheric origin for the narrow emission peak that is often superimposed on a wide platform (see also Hatzes 1995, Fernández & Miranda 1998), while the platform or flat extended emission wings might arise from the circumstellar gas environment.

The different line fluxes between observations taken at different epochs may be due to flaring. Flares are magnetic reconnection events, and can be as short as ~ 1 h, such that their evolution is difficult to trace in non-continuous observations. For this reason the number of flares reported for V410 Tau is quite limited. Most of these events were observed spectroscopically (e.g. Welty & Ramsey 1995), and some flares were detected also in photometric monitoring programs (Rydgren & Vrba 1983, Vrba et al. 1988).

In addition to these well-established activity phenomena observed in the optical, magnetic processes further up in the atmosphere, i.e. the corona, are expected to give rise to radio and X-ray emission. Indeed, the radio emission of V410 Tau is highly variable both in intensity and spectral index (Cohen et al. 1982, Bieging et al. 1984), leading to the conclusion that it must arise from a non-thermal process, probably related to magnetic activity (see Bieging & Cohen 1989 and references therein). Bieging & Cohen (1989) monitored the radio flux density at monthly intervals over one year. They failed to detect strong radio flares, but found evidence for a modulation with a period that is half of the period reported from optical observations. X-ray data of V410 Tau has been presented by e.g. Strom & Strom (1994), Neuhäuser et al. (1995), and Stelzer & Neuhäuser (2001). Costa et al. (2000) has extensively discussed archived *International Ultra-violet Explorer* (IUE) and *ROSAT* observations of this star. Despite its obvious variability in the X-ray regime no direct signs for rotational modulation or X-ray flares have been observed from V410 Tau so far.

The detailed relations among the various atmospheric regions involved in stellar magnetic activity (photosphere, chromosphere and corona) remain unexplained and call for a systematic investigation. Towards this end we organized contemporaneous optical and X-ray observations of V410 Tau. Dedicated photometric as well as intermediate- and high-resolution spectroscopic observations in the optical were planned for a time interval of ~ 11 d, simultaneous to three exposures with the *Chandra* X-ray satellite. This enabled us to study activity on V410 Tau that evolves on short timescales, i.e. rotational effects and flares. In addition we examined historical photometric data of V410 Tau to examine its long-term variability.

We will present our results in a series of two papers. In the present paper we focus on the examination of the relation between emission in various energy bands and the optical rotation cycle, and the long-term photometry, while in a subsequent paper (Fernández et al., in prep.) we will concentrate on the numerous flares found during our campaign. The present paper is structured as follows. In Sect. 2 we present the layout of our observations. We discuss the evolution of the photometric 1.87 d cycle over the years in Sect. 3. This section includes a new de-

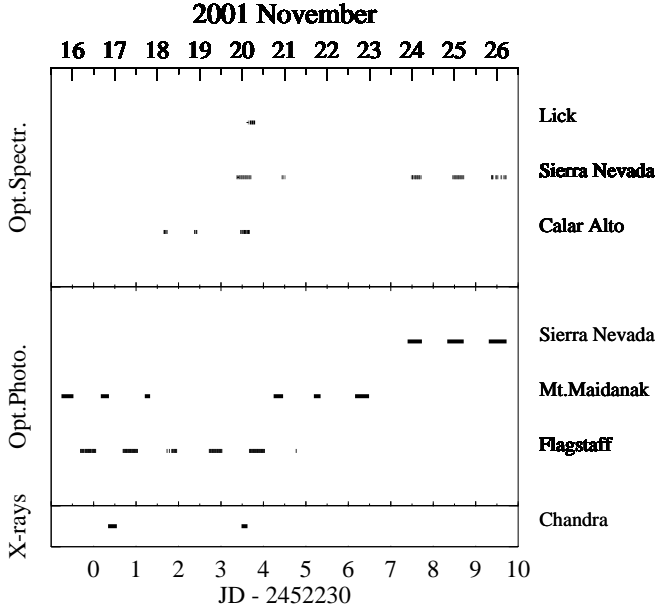


Fig. 1. Observing Journal for our monitoring of V410 Tau in Nov 2001. Note, that our campaign includes a third *Chandra* observation which was performed in March 2002 and is not shown in this diagram.

termination of this period and the ephemeris for the minimum brightness, and the tentative detection of an activity cycle. The relation between spots and various activity diagnostics are examined in Sect. 4. We devote Sect. 5 to the description of the X-ray spectrum of V410 Tau. The results are discussed in Sect. 6. Sect. 7 presents a brief summary.

2. Observations and Data Reduction

Simultaneous optical and X-ray observations were planned for V410 Tau from Nov 15 to 26, 2001 (UT). Optical photometry and spectroscopy were carried out from several observatories (see below) while three X-ray observations were scheduled with *Chandra* using the Advanced CCD Imaging Spectrometer for Spectroscopy (ACIS-S). Our observing strategy was to maximize the probability of detecting large amplitude variability in the X-ray observations. If the X-ray emission comes from spotted regions the maximum of the X-ray emission should occur at the minimum of the optical lightcurve, i.e. at phases when the spot is on the visible hemisphere, and vice versa. Therefore, the *Chandra* observations were scheduled for the time near minimum and maximum of the known rotation cycle, respectively.

Nevertheless, the third *Chandra* observation was delayed by several months because at the anticipated time in November 2001 the satellite had to be shut down due to high solar activity. Therefore, optical data is available only for the first two *Chandra* observations. The complete observing log for the campaign in Nov 2001 is given in Fig. 1. In the following the individual observations and the data reduction are described.

2.1. Optical photometry

2.1.1. Sierra Nevada

The photometric observations carried out at the Observatory of Sierra Nevada (Granada, Spain) were performed with a Strömgen photometer attached to the 90 cm telescope. The photometer is equipped with identical six-channel *wby* spectrograph photometers for simultaneous measurements in *wby* or the narrow and wide $H\beta$ channels (Nielsen 1983). We carried out *wby* measurements. Integration times were 60 s for V410 Tau and for its two comparison stars, HD 27159 and HD 283561, as well as for the background sky. Differential photometry was carried out during all the photometric nights, except during the last one, in which the absolute calibration was done.

The error bars of the differential photometry, as estimated from the difference between the two comparison stars, are 0.005 mag in the *u* band and less than 0.001 mag for the *vby* bands. Nevertheless, we note that both comparison stars are about two magnitudes brighter than V410 Tau, therefore, slightly larger errors are expected for the target star. For the absolute photometry, the residuals of the standard stars (difference between computed and published values) are less than 0.026 mag for the *V* band and less than 0.008, 0.010 and 0.017 mag for the (*b* - *y*), *m*1 and *c*1 indexes, respectively.

2.1.2. Mt. Maidanak

Diaphragm photometry was performed at the Mt. Maidanak Observatory, Uzbekistan. All observations were obtained with the 48 cm telescope equipped with a one-channel pulse-counting photometer. We carried out Johnson *UBVR* measurements with a 28'' diaphragm. A detailed description of the equipment and measuring techniques was given by Shevchenko (1980). The exposure time was typically 40-120 s, depending on the band and sky-background brightness. As a rule, seven standard stars from the list of Landolt (1992) were observed on each night to determine the atmospheric extinction coefficients. The instrumental photometric system was reduced to the standard system by the method of Nikonov (1976). The star BD+28 643 was used as a secondary standard. The rms error of a single measurement on a moonless night was 0.032, 0.007, 0.005, and 0.005 mag in *U*, *B*, *V*, and *R*, respectively.

2.1.3. USNO Flagstaff

Observations from the USNO, Flagstaff Station (NOFS, USA) used the NOFS 1.0m f/7.3 R/C telescope along with a SITE/Tektronix 2048 × 2048 CCD. A mask around the CCD limits its usable area to 1815 × 1815 pixels, or about 20 × 20'. By positioning V410 Tau in one corner of the array the largest number of candidate comparison stars could be included. Several nights prior to the campaign, plus the photometric nights during the campaign, were used to calibrate all potential comparison stars in the field. *UBVR_cI_c* filters were used, along with a large number of Landolt standard stars (see Landolt 1983 and Landolt 1992), to calibrate the comparison

stars. Five of the potential comparison stars were found to be constant during the survey interval, and bright enough to give reasonable signal-to-noise (S/N) for differential photometry. Differential photometry at $UBVR_cI_c$ was performed extensively on the five nights Nov 16 through Nov 20 UT, plus a few data points on nights prior to and subsequent to this period.

2.2. Optical spectroscopy

2.2.1. Intermediate-resolution Spectroscopy

Intermediate resolution spectroscopy was carried out at the 1.5m telescope on the Observatory of Sierra Nevada (Granada, Spain) using the spectrograph ALBIREO (see Sanchez et al. 2000) in long-slit mode. The detector was a EEV8821/T CCD of 1152×770 pixels with a $22.5 \mu\text{m}$ pixel size. Observations were done on two spectral ranges: 4000–5160 Å (blue) and 5645–6790 Å (red). The full width half maximum (FWHM) of the lines of the calibration lamps were 1.7 Å and 1.5 Å for the blue and red ranges, respectively. Several spectrophotometric standard stars were observed on the three photometric nights, with the aim of correcting the slope of the continuum but no flux calibration. A set of templates, with spectral types ranging from K2 to K5 were also observed.

The data reduction and analysis was done with the *longslit* package of IRAF (Image Reduction and Analysis Facility¹). The longslit tasks were required due to the strong distortion of the sky lines along the spatial direction. Individual spectra have a S/N of about 30.

2.2.2. High-resolution Spectroscopy

High-resolution spectroscopic observations were performed using the Fiber Optics Cassegrain Echelle Spectrograph (FOCES) and a 2048×2048 pixel SITe CCD attached to the 2.2m telescope at the Calar Alto Observatory (Almeria, Spain). The spectra include some seventy orders, covering a range from 4200 Å to 7000 Å, with a nominal resolving power of $\lambda/\Delta\lambda \approx 30\,000$. Technical details regarding FOCES can be found in Pfeiffer et al. (1998).

Additionally, high-resolution spectra were taken at the University of California’s Lick Observatory on Mt. Hamilton using the Hamilton echelle spectrograph on the 3m-Coude telescope. The instrument yielded 107 spectral orders spanning a wavelength range of $\sim 3500 - 10000$ Å. A thinned Ford 2048×2048 pixel CCD with $15 \mu\text{m}$ pixel size was used. Using an aperture plate above the slit gave a slit width of $640 \mu\text{m}$, corresponding to $1.2''$ projected on the sky, and ~ 2 pixels on the CCD. This gave a 2-pixel spectral resolution of ~ 0.1 Å FWHM (i.e., 2-pixel $R \approx 60000$).

All high-resolution spectra have been reduced and extracted using the standard IRAF reduction procedures (bias subtraction, flat-field division and optimal extraction of the

spectra). Wavelength calibration was done using spectra of a Th-Ar lamp. Finally, for each order we normalized the extracted spectra by means of a polynomial fit to the observed continuum.

2.3. X-rays

The *Chandra* observations were performed with V410 Tau on the back-illuminated ACIS-S3 CCD. In order to avoid pile-up (the detection of more than one photon as a single event which leads to distortion of the spectral shape and underestimation of the count rate) the source was placed $4'$ off the aim-point. This way, for the expected X-ray brightness of V410 Tau in the *Chandra* energy band, pile-up should be below 10 %. However, we performed additional checks on the count rate and the spectrum to verify that pile-up is negligible (see Sect. 5). Our data analysis is based on the events level 1 data provided by the pipeline processing at the *Chandra* X-ray Center (CXC), and was carried out using the CIAO software package² version 2.3.

In the process of converting the level 1 events file to a level 2 events file for each of the observations we performed the following steps: We filtered the events file for event grades (retaining the standard ASCA grades 0, 2, 3, 4, and 6), and applied the standard good time interval (GTI) file. Events flagged as cosmic ray afterglow were retained after inspection of the images revealed that a substantial number of source photons erroneously carry this flag. We also checked the astrometry for any known systematic aspect offsets using CIAO software, and performed the necessary corrections by updating the FITS headers.

To find the precise X-ray position of V410 Tau we ran the *wavdetect* source detection routine (Freeman et al. 2002). For the source detection we used a binned image of the ACIS-S3 chip with $\sim 3'' \times 3''$ pixels. The significance threshold was set to 10^{-6} , and wavelet scales between 1 and 8 were applied. After V410 Tau was located in this way we extracted the counts from a circular region of $4''$ radius around the position found by *wavdetect*. This area includes $\approx 97\%$ of the source photons (for a monochromatic 1.49 keV source). The background was extracted from an annulus in a source-free region surrounding V410 Tau. The observing log for the three *Chandra* exposures and the average ACIS-S count rates of V410 Tau in the 0.2 – 8 keV energy range are given in Table 1.

3. Variability in the Optical

The rotational period of V410 Tau was first determined by Rydgren & Vrba (1983), who found a value of 1.92 d from photometric data obtained over a 6-day interval. Vrba et al. (1988) combined data taken during five observing seasons between 1981 and 1987, and improved the measurement of the period. Only one year later Herbst (1989) noted a linear trend present in the $O-C$ (observed minus computed) diagram for minimum light of V410 Tau based on the ephemeris by Vrba et al. (1988)

¹ IRAF is distributed by the National Optical Astronomy Observatories, which is operated by the Association of Universities for Research in Astronomy, Inc. (AURA) under cooperative agreement with the National Science Foundation.

² CIAO is made available by the CXC and can be downloaded from <http://cxc.harvard.edu/ciao/download-ciao-reg.html>

Table 1. Observing log for the three *Chandra* ACIS-S observations of V410 Tau. Rotational phases are computed using the new ephemeris given in Table 2. Values refer to the 0.2 – 8 keV energy band.

Seq.#	Start Date [d/m/y h:m]	Exp. Time [s]	ϕ_{rot}	Rate [10^{-3} cps]
200130	16/11/01 20:11	14925.3	0.91 – 1.00	296 ± 4
200190	19/11/01 23:37	11007.6	0.58 – 0.65	361 ± 6
200191	07/03/02 06:16	17734.2	0.89 – 0.99	324 ± 4

indicating the need for a further revision. The most recent and most widely used ephemeris for the photometric minimum of V410 Tau is the one presented by Petrov et al. (1994): $\text{JD}(\text{min}) = \text{JD } 2446659.4389 + 1.872095(\pm 0.000022) \text{ E}$. This result is based on data from 1986–1992.

We have used this period and ephemeris to phase-fold the photometry from November 2001, and found that the minimum is offset from phase $\phi = 0$ by $\Delta\phi \sim 0.14$ (Stelzer et al. 2002). A shift of the optical minimum with respect to the ephemeris given by P94 had already been identified by Grankin (1999) in his investigation of seasonal lightcurves acquired within the last decade. Our measurement continues the monotonic trend observed since 1990. This migration of the minimum could either indicate a change in the latitude of the spots or the need for a new estimate of the period. The structure of the lightcurve of V410 Tau undergoes changes over the years (Fig. 3 and Sect. 3.3) suggesting that indeed the distribution of surface features is variable in time. However, spot models based only on photometric data cannot provide unique information about the shape and latitude of the spots.

3.1. Migrating Spots and Differential Rotation

As outlined above, the systematic phase shift of the minimum observed over the last ~ 10 yrs could be due to a latitudinal migration of the spots on the differentially rotating surface. The differential rotation of V410 Tau is known from Doppler Imaging, where the differential rotation parameter $\kappa = \Delta\Omega/\Omega_{\text{eq}}$ (Ω_{eq} is the rotation rate at the equator) for an assumed solar-like rotation law was found to be ≈ 0.001 (Rice & Strassmeier 1996). This value is much smaller than the solar differential rotation which is ≈ 0.2 from equator to pole (Snodgrass 1983), but not untypical for a fast rotating star (see e.g. Collier Cameron 2002).

The phase shift accumulated over the last decade with respect to the ephemeris by P94 is $\Delta\phi \approx 0.14$ (see Stelzer et al. 2002). This indicates that $\Delta P/P \approx 6 \times 10^{-5}$. If we assume a solar rotation law, and that the major spot was centered on the pole initially ($\theta_1 = 90^\circ$), this change in period implies that the spot should have moved to a latitude of $\theta_2 \approx 75^\circ$ by 2001. However, such a large displacement is clearly inconsistent with the relatively unchanged shape of the photometric lightcurve. Furthermore, Doppler maps obtained in the years

Table 2. Ephemeris of V410 Tau: value by P94 and our update.

Reference	T_{min} [JD]	P_{rot} [d]
P94	2446659.4389	1.872095 ± 0.000022
here	2452234.285971	1.871970 ± 0.000010

1990 to 1994 seem not to show a systematic movement of the main spot.

3.2. An Update of the Period and Ephemeris

In this section we examine the second possibility for the observed systematic shift of the minimum in the optical lightcurve, namely the need for a refinement of the value for the rotational period. In the following, whenever we refer to the ‘rotational period’ or ‘rotation cycle’ the reader should keep in mind that this is the period representative for the main spot that dominates the observed lightcurve.

For our update of the period we made use of historical data from the T Tauri photometry data base.³ We split the available *V* band photometry on a yearly basis, and derived the most significant period for each of the observing intervals using the string length method (Dworetsky 1983). Each seasonal lightcurve was folded with its period to determine the time of minimum T_0 by fitting a polynomial to the folded lightcurve. We used the value for the period given by P94 to compute the number of cycles elapsed between each of the seasonal points T_0 and the time of minimum observed by us in November 2001, using this last observation as a reference point. Then we computed the $O - C$ diagram for the minima T_0 as a function of cycle number. The residuals in this diagram can be minimized by modifying the period. But the $O - C$ residuals show systematic non-linear trends for data acquired before 1990. The large scatter for these earlier years may indicate that the spots migrated in an irregular way on the surface of V410 Tau. For years later than 1990 we observe a monotonic trend in the $O - C$ residuals. Therefore we used only observations obtained in 1991 and later for the final determination of the period. This way a best fit period of $1.871970(10) \text{ d}$ is found (see Table 2 for the new ephemeris of V410 Tau), slightly lower than the earlier determination by P94 which was based on data from 1986 to 1992. The residuals in the $O - C$ plot for the new best fit period are shown in Fig. 2. In the following we use the ephemeris and period newly derived here.

3.3. Changes in the spots

Provided the newly derived ephemeris represents the correct period for the surface structure on V410 Tau, the minima of phase folded lightcurves for each observing season should now coincide with $\phi = 0$. This is verified in Fig. 3 where the phase plots of the yearly averages of the *V* band lightcurve of V410 Tau since 1981 are shown. Photometry from earlier years

³ The T Tauri photometry data base is compiled and maintained by W. Herbst and available at <http://www.astro.wesleyan.edu/~bill/>

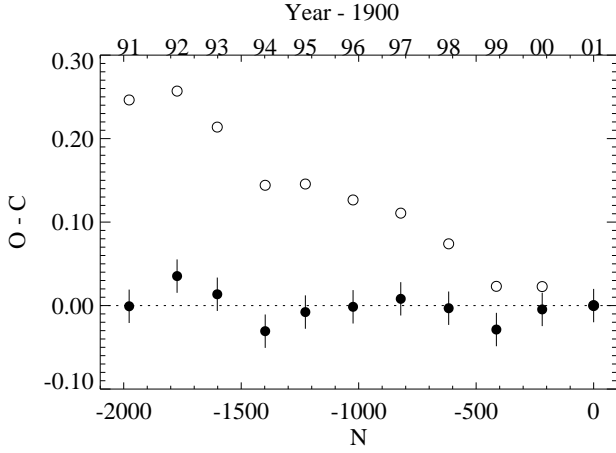


Fig. 2. $O - C$ diagram for the seasonally averaged times of minimum T_0 in the V band lightcurve of V410 Tau versus rotational cycle number N . *Open circles* - for the period given by P94, and *filled circles* - after adapting the period to minimize the residuals. Data obtained in Nov 2001 were used as reference point.

is available only in graphical form, and the time information can not be extracted accurately enough for studies of the 1.87 d periodicity (original references Romano 1975, Rössiger 1981).

The minima of all years included in our determination of the period, i.e. 1990 to 2001, are aligned at the same phase, as expected. The minima of the years 1986 and 1989 do show a shift. This phase migration seems to be irregular and may indeed indicate changes in the spot location or distribution. Between 1981 and 1985 the lightcurve of V410 Tau was characterized by a completely different, double-peaked structure. Data from these years has been extensively discussed by Herbst (1989) who showed that a two-spot model provides a good description of the visible lightcurve.

Changes in the shape of the lightcurve reflect variations of the structure of active regions. In order to quantify these changes we plot the time-evolution of amplitude, mean, minimum, and maximum of the V band lightcurve in Fig. 4. Over the years the lightcurve of V410 Tau has systematically become more stable and its variability more regular.

From a simple harmonic fit to the mean V band magnitude for data obtained after 1990 (also displayed in Fig. 4) a tentative cycle length of 5.4 yr is derived. Inspection of the photometry in other bands, also available at the T Tauri photometry data base, shows the same 5.4-yr-pattern in the B band with a similar amplitude, supporting the idea that this variation can be attributed to a spot activity cycle. The data in the R and I band is scarce and inhomogeneous because of the use of different filters (Johnson and Cousin).

However, when extrapolating the 5.4 yr-periodicity to earlier years (dotted line in Fig. 4) the data first runs out of phase with the 5.4 yr period and then turns into completely irregular behavior. The evolution of both the shape of the lightcurve and the mean brightness are suggestive of a transition towards less active behavior.

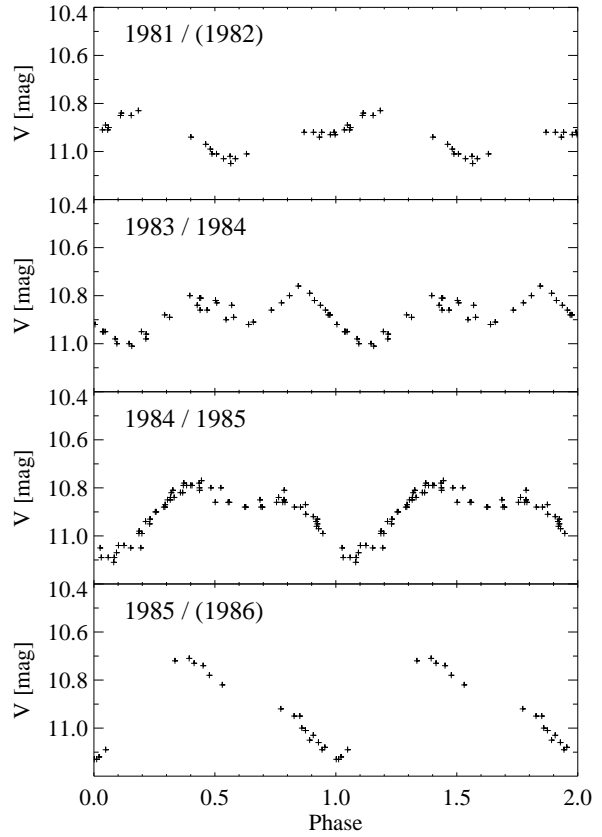
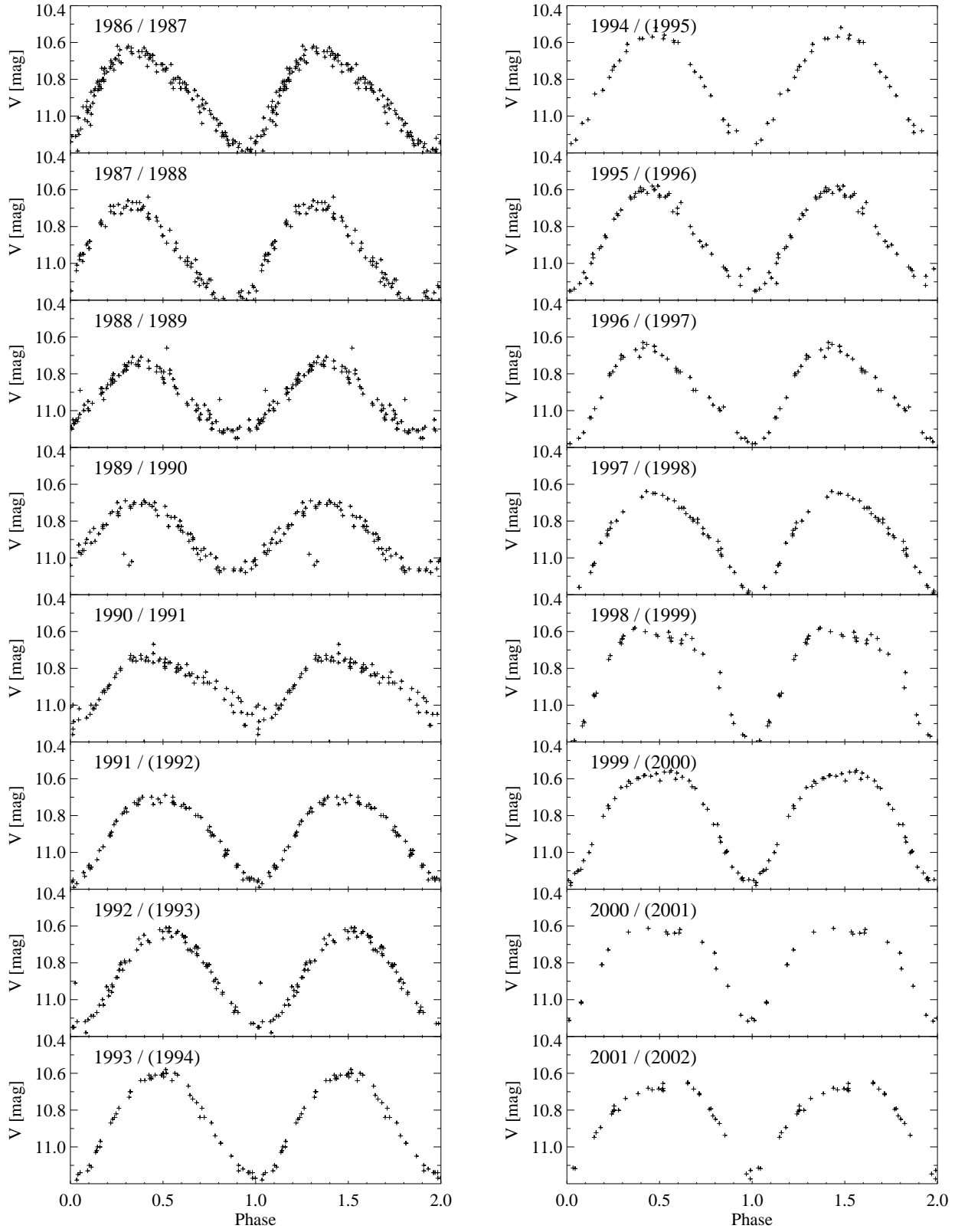


Fig. 3. Seasonally averaged V band lightcurves of V410 Tau from 1981 to 2001 phase folded with the new ephemeris given in Table 2 (continued on the next page). Data are extracted from the data base maintained by W. Herbst. The data for 2001 was obtained by one of us (KG) in the months prior to our coordinated observing campaign.

4. Simultaneous X-ray and Optical Data

A major aim of this campaign was to study simultaneous X-ray and optical observations in order to look for correlations, in particular those related to the spot rotation cycle. To this end the *Chandra* observations were purposely scheduled to cover different rotational phases of the star. If X-ray emission is related to spotted regions the maximum of the X-ray emission should occur at the minimum of the optical lightcurve, i.e. at times when the spot is on the visible hemisphere, and vice versa. Therefore, to maximize the amplitude of the expected X-ray variability we observed near optical maximum and minimum. In addition our spectroscopic optical monitoring provided information on the time-evolution of the $H\alpha$ line and the radial velocity (RV).

The V band lightcurve obtained during our monitoring in November 2001 is shown in the lowest panel of Fig. 5 phase-folded with the new period and ephemeris. The differential photometry carried out in the Strömgren system was transformed to the Johnson system with help of the absolute Strömgren photometry done during the last night. We point out that the photometric measurements from the three observing

Fig. 3. *continued*

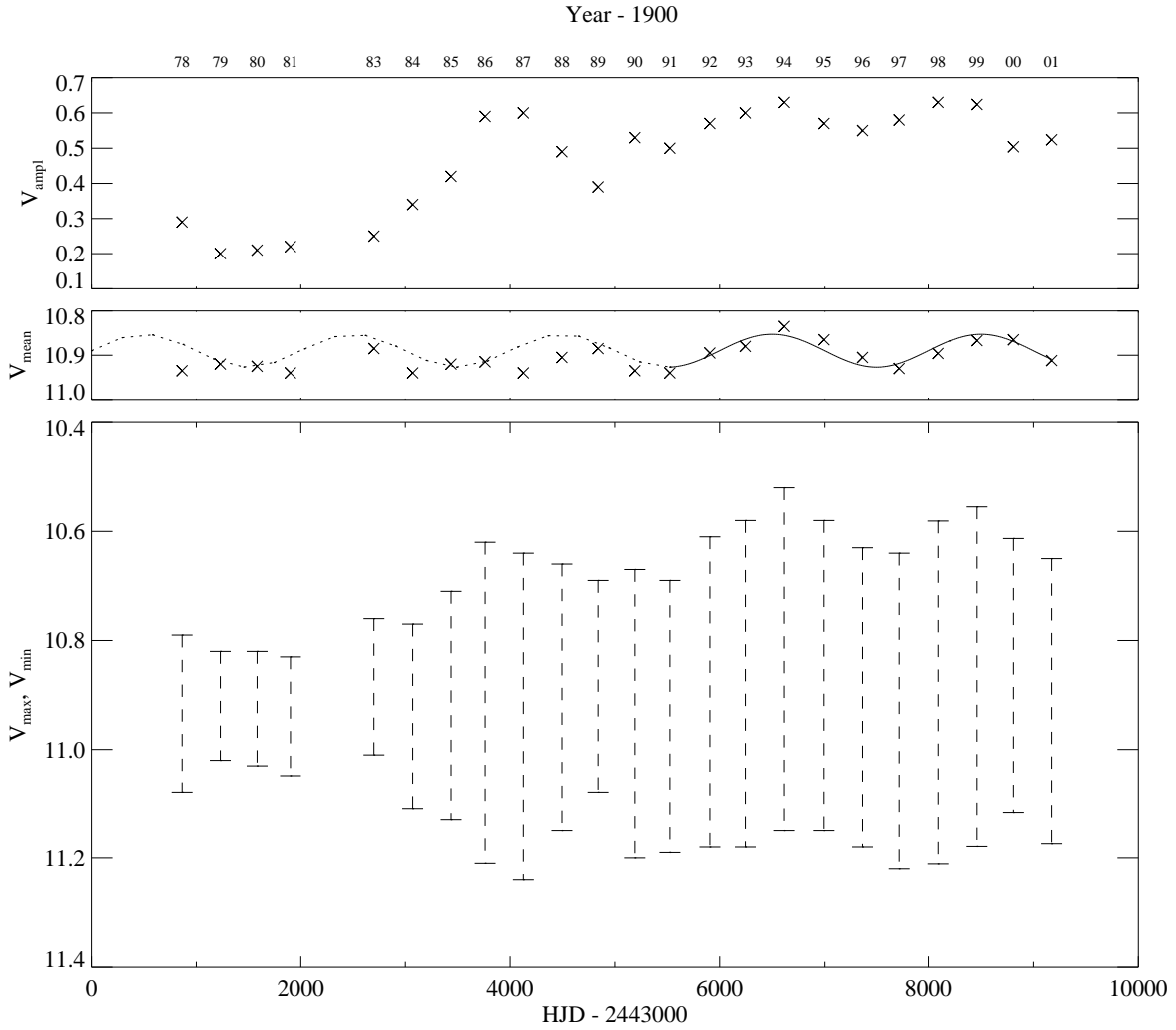


Fig. 4. Longterm behavior of amplitude, mean, and maximum and minimum of the V band lightcurve of V410 Tau from 1978 to 2001. Data points represent seasonal averages. The numbers on the top y-axis stand for the year in which the observing season started.

sites complement each other to provide nearly full coverage of the rotational cycle despite the relatively short duration of the monitoring (11 d; see Fig. 1). Photometric data in the $UBRI$ bands was also obtained, but does not provide new information on the *phasing* of the 1.87 d cycle. We will use these latter lightcurves for the discussion of flares in an accompanying paper (Fernández et al., in prep). Some of these flares can be seen in the V band lightcurve displayed in Fig. 5. However, our aim in this section is to examine activity parameters for a possible relation to the 1.87 d cycle, and short-term random processes such as flares are not of interest.

4.1. X-rays

The mean ACIS count rates listed in Table 1 indicate that the X-ray emission of V410 Tau was variable. To check the relation with the optical photometry we generated X-ray lightcurves,

and phase-folded them with the 1.871970 d period derived in Sect. 3.2. The result for the two observations obtained in November 2001 is shown in Fig. 5. A rapid rise of the X-ray count rate took place near optical minimum in the observation from November, probably indicating the onset of a flare. This event was not accompanied by simultaneous observations in the optical, but just a few hours later two flares were observed from Mt.Maidanak, hinting at a possible relation between the optical and X-ray emission sites.

A third *Chandra* pointing was obtained in March 2002 near optical minimum, i.e. coinciding in phase with the first November observation. As this observation is not simultaneous with the optical lightcurve we do not display it in Fig. 5. The March data does not show significant time-variability, and its count rate is somewhat higher than the lowest (quiescent) level measured in the November observation taken at the same rotational phase. Thus, while the two November pointings

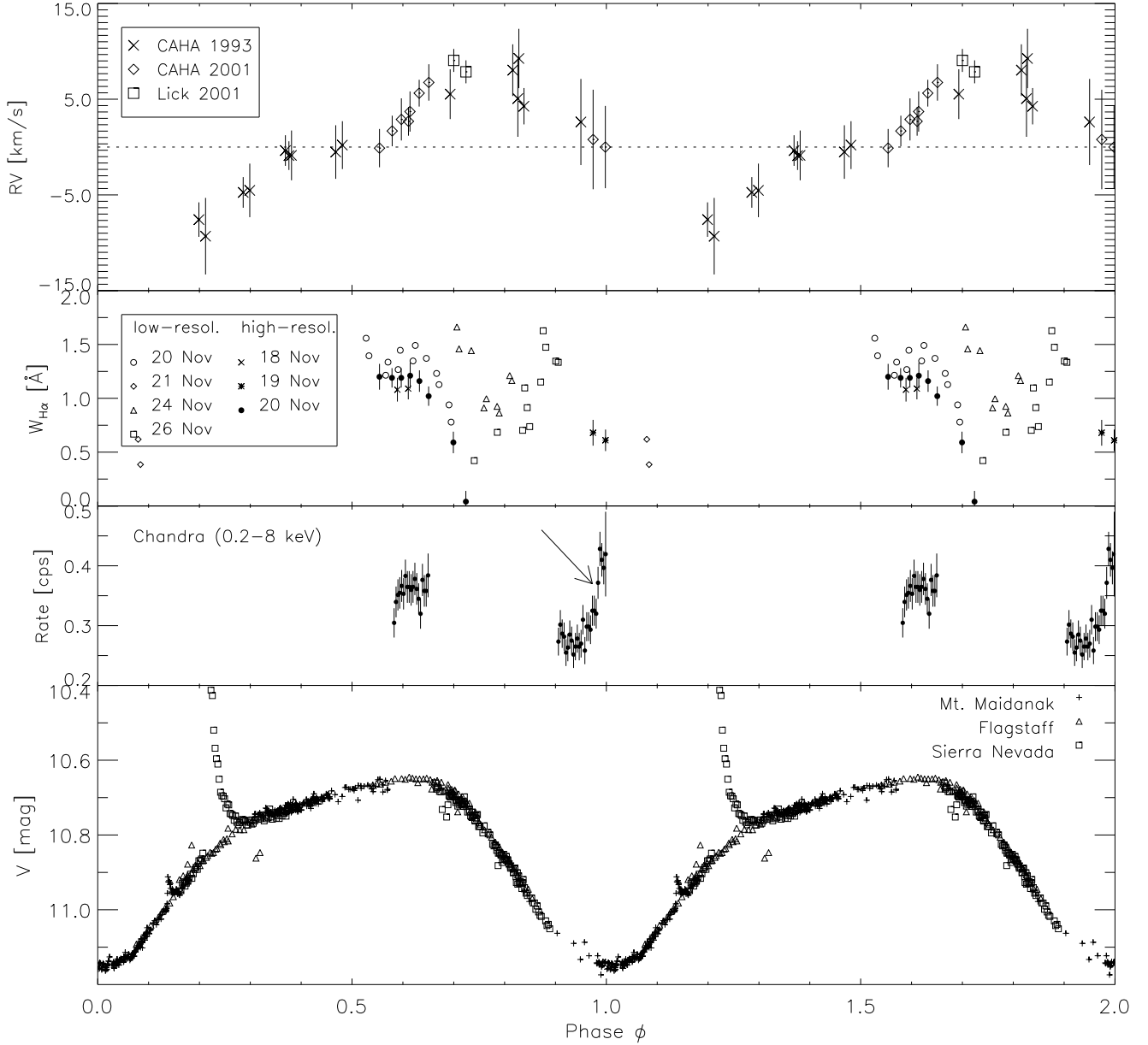


Fig. 5. Multi-wavelength phase plot for the 1.87 d cycle of V410 Tau. From top to bottom: Radial velocity, equivalent width of $H\alpha$, X-ray count rate, and V band photometry. Except for some data points in the radial velocity curve all measurements are obtained quasi-simultaneously in November 2001. The large flare visible in the V band lightcurve was also observed spectroscopically, but the equivalent widths of $H\alpha$ are outside the range displayed in this figure (see Fernández et al., in prep. for a detailed discussion). The fast increase of the X-ray count rate near $\phi = 0$ (marked with an arrow) probably indicates the beginning of a flare (see Sect. 5).

seem to suggest that the X-ray emission depends on rotational phase, this conclusion is not supported by the observation from March.

4.2. $H\alpha$

The $H\alpha$ line is in the spectral range of both the intermediate- and the high-resolution spectra obtained within this campaign. $H\alpha$ is always weak in emission. We display the equivalent

width $W_{H\alpha}$ measured at different phases of the photometric rotation cycle in the second panel of Fig. 5. On Nov 20 both intermediate- and high-resolution spectra were obtained, and the measured equivalent widths are in good agreement within the uncertainties. The error bars for the high-resolution spectra are based on the assumption of an accuracy in the continuum normalization of 10 %. The typical error bar for the values from the low-resolution spectrum are $\sim 30\%$.

On Nov 24 a large flare erupted which we monitored simultaneously in spectroscopy and photometry. Note, that the event is not seen in the equivalent width curve shown in Fig. 5 because the values for $W_{H\alpha}$ measured during the flare are higher than the displayed plot range.

Due to poor weather conditions, the phase coverage of the $H\alpha$ data is limited. While the equivalent width seems to undergo (short-term) changes within each night, no clear trend related to the rotational phase can be found.

4.3. Radial Velocity and $v \sin i$

We derived the RV and the projected rotational velocity ($v \sin i$) from the optical high-resolution spectra using a cross-correlation analysis with several template stars of spectral class K2, K4 and K5.

The value of $v \sin i$ is obtained by comparing the spectra of V410 Tau within several spectral orders to that of a broadened template. Amongst the templates at our disposal, the K2 V star HD 166620 broadened to a velocity of 74 ± 3 km/s gave the best fit. This broadening agrees with the estimates of Vogel & Kuhi (1981) (76 ± 10 km/s), Hartmann et al. (1986) (70.9 ± 9 km/s), and Hatzes (1995) (77 ± 1 km/s).

We estimated the stellar RV from the data acquired in Nov 2001. This was done by averaging measurements that were obtained at phases $0.5 < \phi < 0.6$. The four spectra obtained in this phase interval correspond to the maximum in the lightcurve, and therefore their shape should be less distorted by the spots. Using this procedure we found an average RV of 17.9 ± 1.8 km/s similar to the stellar RV of V410 Tau given in the literature (18 km/s, Herbig & Bell 1988).

The relative shift between photospheric lines was then measured by cross-correlating the spectra of V410 Tau with the spectrum of the template HD 166620. Three different orders have been used, with wavelengths centered at 5400, 6100 and 6400 Å, and a wavelength coverage of 80 Å in each order. A parabolic function was used to find the center and width of the correlation peak, and the errors were computed from the fitted peak height and the asymmetric noise as described by Tonry & Davis (1979). The final RV are an average of those obtained with the three orders, and the accuracies are the combined error bars for each individual measurement.

We performed this procedure for each of the 12 individual high-resolution spectra of V410 Tau obtained during our campaign. The resulting RV curve is shown in the top panel of Fig. 5 as a function of rotational phase, combined with a number of measurements obtained in 1993 and presented by Fernández & Miranda (1998) added here to improve the phase coverage.

From this latter data set we used only the spectrum in the range 6680 – 6730 Å. This spectral range is useful because strong photospheric lines such as the Li I line (6708 Å) are present. In a first step, each of the 16 spectra from 1993 was cross-correlated with the first spectrum of the 1993 series. The position of the maximum of the cross-correlation function gives then for each spectrum the average shift of the photospheric lines relative to the first one. To be able to combine these results with the RV measurements obtained during 2001 we took the velocity shift at rotational phase $\phi = 0.5$ as a zero-point. At this phase the photometry shows that the star is at its brightest, and thus the spot(s) or a large part of it is not visible. As a consequence, we expect to see the normal stellar photosphere, and the velocity shift should be equal to the stellar RV, i.e. $\Delta V_{\text{rad}} = 0$.

From Fig. 5 it is readily seen that the RV varies from ≈ -10 to $+10$ km/s, and the phase shift is ≈ 0.25 when compared with the photometric lightcurve. This phase shift can be understood if the cool spot is responsible for the distortion of absorption lines (Vogt et al. 1987). In this scenario, the RV is large when the spot is near the limb and close to zero when the spot is face-on ($\phi \approx 1.0$) or occulted by the star ($\phi \approx 0.5$). This result shows how magnetic stellar activity can affect the spectroscopic search for very low-mass companions orbiting around PMS stars.

5. X-ray Properties

We extracted an X-ray spectrum for each of the three *Chandra* pointings. The observation from Nov 16/17 shows a pronounced increase in count rate at the end of the exposure (discussed above in Sect. 4.1). If this behavior in the X-ray lightcurve is due to a flare, it is expected that the spectrum changes as a consequence of coronal heating. To unveil any eventual spectral variability in the data we split the Nov 16/17 observation into a quiescent and flaring part, separating the data at JD 2452230.4870 (marked with an arrow in Fig. 5). No systematic trend is seen in the temporal behavior of the other two *Chandra* pointings. Therefore, we think of both as representing the quiescent, i.e. non-flaring, state of V410 Tau.

As outlined in Sect. 2.3 we avoided excessive photon pile-up by placing V410 Tau at an off-axis angle of $\sim 4'$. To check whether any remaining pile-up affects the spectrum the source extraction area was varied: Next to the spectrum from a $4''$ radius centered on the *wavdetect* position of V410 Tau we extracted the spectrum from an annulus where we excluded the inner source region. In the outer portions of the PSF the count rate is smaller and no pile-up is expected. Visual inspection does not show any distortion of the full-source spectrum with respect to the one extracted from a (with certainty pile-up free) annulus. The supposition that pile-up is negligible was confirmed when we fitted both spectra with the same model and found no significant differences in the spectral parameters. In the following we describe the details about our spectral model.

Spectral fitting was done in the XSPEC environment (version 11.2.0). To make up for the continuous degradation of the ACIS quantum efficiency we applied the *acisabs* model

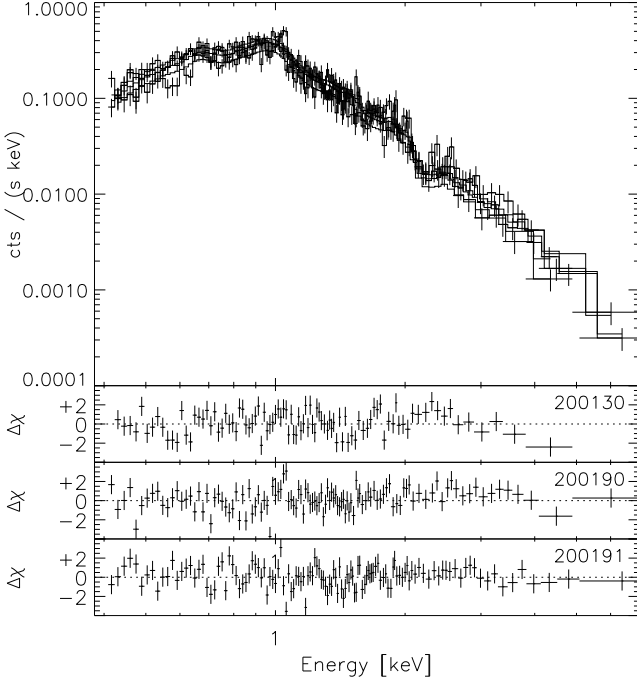


Fig. 6. Quiescent X-ray spectrum of V410 Tau during three *Chandra* exposures. A flare has been eliminated from Obs. Seq.# 200130. The data are overlaid by the best fit model from Table 3. The residuals for each observations are shown in separate panels.

to the auxiliary response file (arf) before loading the data into XSPEC.

We applied the MEKAL model (Mewe et al. 1985) for thermal emission from an optically thin, hot plasma plus a photo-absorption term. Comparison of the three quiescent spectra (first part of Nov 16/17, Nov 19/20, and Mar 7) shows that their spectral shape is very similar. Separate fitting led to indistinguishable parameters. Therefore, we present here the result of a joint modelling of all three quiescent spectra which improves the statistics. To represent the observed small offsets in the flux of the three spectra we allowed for an independent normalization constant.

An acceptable fit ($\chi^2_{\text{red}} \sim 1$ and flat residual) requires a minimum of three MEKAL components, and free elemental abundances. The individual spectra, the best fit model and residuals are displayed in Fig. 6. In Table 3 we summarize the spectral parameters observed during the quiescent state.

To examine whether the rise in the lightcurve on Nov 16/17 represents a heating event we make use of hardness ratios. Hardness ratios are defined as follows:

$$HR = \frac{B1 - B2}{B1 + B2} \quad (1)$$

where $B1$ and $B2$ denote the count rates in a hard and a soft band, respectively. We defined two hardness ratios for the spectral range of ACIS: $HR1$ based on the range from 0.2–1.0 keV

Table 3. X-ray spectral parameters of V410 Tau derived from a joint fit to the three ACIS observations that represent the stars’ quiescent state. A constant normalization factor was applied to allow for the observed difference in X-ray brightness between the three data sets: $N_{200190} = 1$, $N_{200191} = 0.91 \pm 0.04$, $N_{200130} = 0.74 \pm 0.04$. Errors are 90 % confidence levels.

Parameter	Unit	Fit result
N_H	$[10^{21} \text{ cm}^{-3}]$	$0.97^{+0.37}_{-0.32}$
kT_1	[keV]	$0.24^{+0.03}_{-0.02}$
kT_2	[keV]	$0.93^{+0.09}_{-0.07}$
kT_3	[keV]	$2.18^{+0.43}_{-0.28}$
EM_1	$[10^{53} \text{ cm}^{-3}]$	$3.02^{+1.01}_{-1.24}$
EM_2	$[10^{53} \text{ cm}^{-3}]$	$2.23^{+1.26}_{-0.80}$
EM_3	$[10^{53} \text{ cm}^{-3}]$	$2.13^{+0.45}_{-0.77}$
Z	$[Z_\odot]$	$0.20^{+0.08}_{-0.06}$
χ^2_{red} (dof)		1.30 (330)

as the soft band, and 1.0–2.0 keV as the hard band. And $HR2$ with 1.0–2.0 keV representing the soft band and 2.0–8.0 keV representing the hard band. In Fig. 7 these hardness ratios are plotted for the four time segments introduced above. A hardening of the spectrum with a significance of $\approx 2\sigma$ is apparent during the second part of the Nov 16/17 observation. This may be seen as an indication that indeed V410 Tau underwent a flare, because flares are a result of (magnetic) heating.

6. Discussion

We have carried out an intensive coordinated monitoring campaign in the optical and X-ray wavelength ranges with the aim to study correlations between the photometric rotation cycle of V410 Tau and different activity diagnostics. Combining our new data with historic photometric measurements we re-examined the variability in the optical lightcurve of V410 Tau on various timescales: (i) spot (rotation) cycle, and (ii) long-term (activity) cycle.

6.1. Variability in the spot rotation cycle

Optical photometric observations were performed at three sites around the globe, thus providing complete phase coverage of the 1.87 d spot cycle despite the short monitoring time of 11 d. This has allowed us to measure the time of the minimum in the V band lightcurve of V410 Tau with high precision. Combining this measurement with lightcurves from the years 1990 to 2001 we derived an update of the rotational period. The need for a revision of the period was indicated by a systematic shift of the times of minimum in seasonally averaged optical lightcurves folded with the most recent ephemeris for V410 Tau given by P94. We attribute this to the fact that P94 based their period

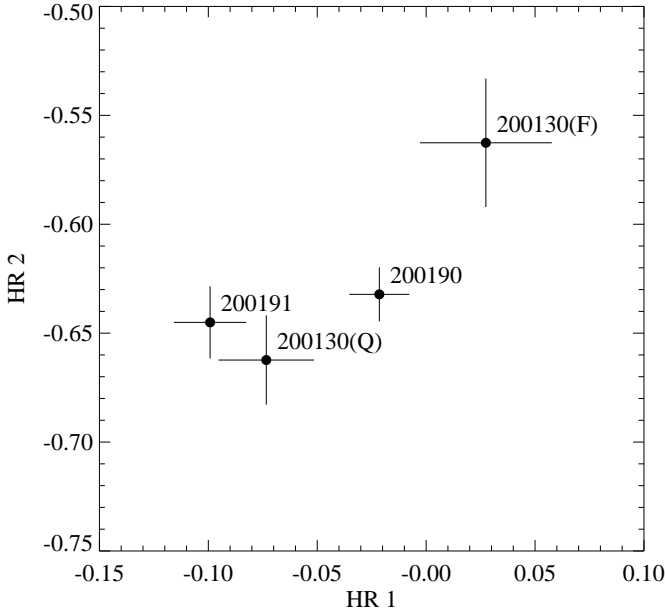


Fig. 7. ACIS hardness ratios for V410 Tau. Flare and quiescent state for observation 200130 are labeled with ‘F’ and ‘Q’, respectively. Error bars denote 1σ uncertainties.

determination on data acquired between 1986 and 1992, where the time of minimum seems to have varied erratically. The new value for the period is slightly smaller than the period given by P94.

An alternative explanation for the monotonically increasing shift of the time of minimum light observed over the last 10 yrs is latitudinal migration of spots on the differentially rotating surface. However, making use of the differential rotation parameter of V410 Tau known from Doppler imaging we find that the associated change in period would correspond to a quite large movement of the spot on the star, which is not supported by the photometry and Doppler images. Therefore we consider this scenario unlikely as an explanation for the systematic effect observed since 1990. Nevertheless, spot migration may be responsible for the irregular shifts of the time of minimum observed in the years before. Unfortunately, no Doppler images are available for these early years. But spot models adapted to the photometric data imply indeed changes in the surface distribution (latitude, longitude, and filling factor) of the spots (Herbst 1989, Bouvier & Bertout 1989).

In our series of high-resolution spectra we detected RV variations which can be explained by the distortions that a spot induces onto the absorption line profiles of a rotating star. In our RV curve we included data obtained in 1993 next to our recent monitoring from Nov 2001. The RV measurements of these two years agree very well in both phase (if folded with the new period) and amplitude demonstrating that the spot distribution has not changed significantly over the last decade. The half-amplitude of the measured variability is $\Delta V_{\text{rad}} \sim 9 \text{ km/s}$. The RV curve of V410 Tau was also mea-

sured by Welty & Ramsey (1995). Their data showed an indication for an increase in amplitude from ~ 6 to $\sim 8 \text{ km/s}$ from 1992 to 1993, while the overall shape remained stable. These small amplitude variations are consistent with the changes in the V band photometry of the same years, and might be related to longterm changes in the spot size.

In recent years detailed RV studies with high-precision have been carried out for mostly solar-type stars with the aim of detecting low-mass (planetary) companions around them (see e.g. Queloz et al. 2001 for a review). However, in active stars spot-related variability may dominate the RV time series, such that the detection of planets is impeded. Therefore, it is important to assess the amount of perturbation induced by star spots. Saar & Donahue (1997) calculated the maximum perturbation of the RV that a spot distribution with a filling factor f_s induces onto a star: $A_s \approx 6.5 \times f_s^{0.9} \times v \sin i$. By their definition f_s characterizes the inhomogeneous part of the spot pattern. If we apply their Eq. 1 (given above) to V410 Tau we derive $f_s \sim 29\%$, an almost perfect match to the actual size of the spot on V410 Tau inferred from Doppler imaging ($\sim 30\%$; Joncour et al. 1994). Our estimate represents the first attempt to extend the Saar-Donahue relation to fast rotating (and very active) stars, and we conclude that this relation seems to hold also in this regime. Furthermore, our result implies that the spot on V410 Tau is significantly non-uniform. Indeed, Doppler images indicate that the major spot is near the pole but not quite identical with a ‘polar cap’.

There seems to be no other component in the RV data besides the spot induced variability. We use the uncertainties in the individual RV measurements ($\sim 3 \text{ km/s}$) to determine an upper limit for the mass of a short-period binary companion possibly hidden in the data. Assuming a circular orbit for the hypothesized companion, we can exclude such objects with a mass of $m \sin i > 0.03 M_\odot$ and a period of 10 d or less. Due to the short timescale of our monitoring no information can be obtained about longer period companions.

6.2. Detection of an activity cycle ?

Inspection of the V band lightcurves of V410 Tau observed during the last two decades indicates that its behavior has become systematically more stable and its variability more regular: The first photometric data set which provides precise information on both the observing time and the magnitude is from 1981. Around this time a distinct double-peaked structure evolved, which smoothly transformed itself into a single-peaked lightcurve over the following five years. This change went along with an increase in the amplitude by a factor of 2 – 3. Since then the simple near-to sinusoidal shape of the lightcurve has persisted, only subject to comparatively small variations. The most obvious variation within the last ten years is the systematic pattern seen in the mean amplitude. From a simple harmonic fit to the seasonal averages of the V band magnitude of the years 1990 to 2001 a periodic variation of 5.4 yr length is suggested that might represent an activity cycle.

Baliunas et al. (1996) have outlined a connection between the ratio of cycle and rotation periods, $P_{\text{cyc}}/P_{\text{rot}}$, with the dynamo number, D , measuring the efficiency of the stellar dynamo. According to stellar dynamo theory D is directly proportional to $1/P_{\text{rot}}$. From observations of chromospherically active, slowly rotating stars they found that the empirical slope in the $\lg(P_{\text{cyc}}/P_{\text{rot}})$ versus $\lg(1/P_{\text{rot}})$ diagram is ≈ 0.74 . Interpreting the 5.4 yr-variability of V410 Tau as a cycle period we find that its location in the $\lg(P_{\text{cyc}}/P_{\text{rot}}) - \lg(1/P_{\text{rot}})$ -diagram is consistent with the extrapolation of the line identified by Baliunas et al. (1996) into the regime of fast rotating stars. This result is remarkable because it seems to indicate that the dynamo process on PMS stars is very similar to that on more evolved stars. To the best of our knowledge V410 Tau is the first PMS star investigated in this respect.

To extend the comparison with the evolved stars we examined the position of V410 Tau in the $\lg(\omega_{\text{cyc}}/\Omega_{\text{rot}}) - \lg R_0^{-1}$ -diagram, where $R_0 = 2\tau_{\text{conv}}\Omega_{\text{rot}}$ is the Rossby-number, and τ_{conv} the convective turnover time. Saar & Brandenburg (1999) derived τ_{conv} for their sample of chromospherically active stars (mostly objects from the Mt. Wilson Ca II H+K survey) from the models of Gunn et al. (1998), and identified three branches in this plot: inactive, active, and superactive stars. To estimate τ_{conv} for V410 Tau we compare its stellar parameters to the PMS calculations by Ventura et al. (1998), and find $\lg \tau_{\text{conv}} [\text{d}] \approx 2.3$. Because we have found agreement within 0.2 dex between zero-age main sequence convective turnover times estimated from models by Ventura et al. (1998) and those from models by Gunn et al. (1998), we can now make valid comparisons between V410 Tau and main-sequence stars. We find that the location of V410 Tau is not consistent with any of the regions defined by the evolved stars in the $\lg(\omega_{\text{cyc}}/\Omega_{\text{rot}}) - \lg R_0^{-1}$ -diagram. This is presumably due to its fast rotation combined with a large convective turnover time, which is a consequence of its PMS nature. Indeed, most PMS stars – typically characterized by $P_{\text{rot}} \leq 10 \text{ d}$ and $\tau_{\text{conv}} \sim 60 \dots 400 \text{ d}$ – are expected to lie to the right of the active/inactive branches in this diagram ($\lg R_0^{-1} \geq 2$), and below these branches. Given their generally fast rotation only very short cycle periods would place them at the extension of these lines.

V410 Tau is younger ($\sim 1 \text{ Myr}$) than all other stars for which activity cycles have been reported so far, representing a unique test case for dynamo action on the PMS. Among the stars that seem to display cyclic behavior it comes closest to the young solar-analogs, such as AB Dor, EK Dra, and LQ Hya, which are single stars characterized by an age of $\sim 50\text{--}80 \text{ Myr}$, spectral type of early K, and fast rotation ($P_{\text{rot}} < 3 \text{ d}$). A cycle length for AB Dor of 5.3 yr was given by Amado et al. (2001). Berdyugina et al. (2002) identified three cycles of 5.2, 7.7, and 15 yr duration in LQ Hya. The photometry of EK Dra indicates longterm fading over the last 35 years (Fröhlich et al. 2002), while Saar & Brandenburg (1999) have predicted cycle periods of 1.4 and 39 yr for this star.

The observation of activity cycles in young stars is of paramount importance for the understanding of the dynamo operating in these objects. The solar-type $\alpha\Omega$ -dynamo is thought

to be localized in the overshoot layer at the bottom of the convection zone. But in stars with deep convective envelope a ‘distributed’ dynamo located throughout the convective layer may take over. Furthermore, both observations and theory agree in that differential rotation is suppressed in fast rotating young stars (Henry et al. 1995, Küker & Rüdiger 1997). Therefore, the α -effect should dominate over the rotational shear, and a pure $\alpha\Omega$ -dynamo is unlikely to hold. The type and stability of the dynamo solutions depend critically on the strength of differential rotation. For small values of the differential rotation non-axisymmetric modes are preferred (Moss et al. 1995). These modes seem not to oscillate (Küker & Rüdiger 1999) and are difficult to reconcile with the possible observation of an activity cycle on V410 Tau. In fact, the apparent absence of such cycles in PMS stars is usually taken as evidence for the action of a non-solar dynamo.

However, Kitchatinov et al. (2001) have shown that a transition of the dynamo mode takes place at an age of $\sim 5 - 10 \text{ Myr}$, such that in the older stars an axisymmetric oscillating field is preferred. The age of V410 Tau is close to this critical range, indicating that it may be a transition object. This might explain the presence of an activity cycle (representative for oscillating fields) in conjunction with long-lived spots (indicating very stable field structures).

Our present knowledge draws a complicated picture for the magnetic activity of V410 Tau, and PMS stars in general. We stress that our conclusions rely on the observation of just one tentative cycle period. The systematic pattern in the seasonally averaged mean magnitude seems to have its onset a few years before 1990, at the same time when the single-peaked lightcurve developed. Earlier than ~ 1986 the lightcurve shows no signs for cyclic variability. Indeed, in years of low amplitude the V band magnitude assumes an intermediate level, while a value near maximum would be expected if a decrease in spot size and number during a cycle minimum were responsible.

6.3. Spot Rotation Cycle and Activity Diagnostics

Simultaneously with the optical photometric lightcurve we have acquired *Chandra* X-ray observations and optical spectroscopy. *Chandra* has targeted V410 Tau twice during our campaign, at minimum and maximum optical brightness, respectively. Different count levels were found, but their relation to the rotation cycle was not confirmed by a following measurement carried out some months later that showed an intermediate count rate although obtained at the same phase as one of the observations from Nov 2001. A seeming lack of a correlation between X-ray and optical emission was already pointed out by our analysis of archived *ROSAT* data (Stelzer et al. 2002): we found that the count rates varied from one observation to the other, however, without clear relation to the rotation cycle. Similarly the $H\alpha$ equivalent width seems not to show a trend related to the rotational phase. Unfortunately, we were not able to obtain full phase coverage in the optical spectroscopy due to poor weather conditions.

Reports on coordinated multi-wavelength monitoring of PMS stars are scarce in the literature. Multi-wavelength obser-

vations of TTS in the Taurus star forming region using *ROSAT* jointly with optical telescopes have revealed flares in Balmer lines and in X-rays (Guenther et al. 2000). But due to unfortunate conditions during none of these events was observed simultaneously in both the optical and the X-ray range. In the same study a weak correlation between the X-ray and $H\alpha$ emission was seen for the wTTS V773 Tau, suggestive of a relation between the emission sites. Simultaneous X-ray and optical observations of BP Tau were discussed by Gullbring et al. (1997). No signs for any correlation between the optical and the X-ray emission was seen: Two optical flares had no counterpart in X-rays, and the data set did not allow them to examine variations related to the rotation of the star. However, BP Tau is a cTTS, such that variability (in both optical and X-rays) may be induced by accretion. Therefore, it may not be directly comparable to V410 Tau which is a non-accreting wTTS where all variability should be related to magnetic activity similar to more evolved stars.

Recently, Jardine et al. (2002) have modeled the X-ray emission of AB Dor, for which Kürster et al. (1997) did not find any evidence for rotational modulation of the X-ray emission during monitoring with *ROSAT*. The model of Jardine et al. (2002) is based on Zeeman Doppler maps of the surface magnetic field structure, and predicts little rotational modulation of the X-ray emission due to the extended structure and/or high latitudes of coronal features. AB Dor is characterized by dark spots at all latitudes (Donati & Collier Cameron 1997). On V410 Tau the dominant spot seems to be located near the pole, although not completely symmetrically (Hatzes 1995). But the absence of rotational modulation in the X-ray emission of V410 Tau is consistent with a symmetric distribution of X-ray flux with respect to the rotation axis. Therefore, the spot may not be the main site of X-ray production.

6.4. Relation between X-ray and $H\alpha$ flux

Coronal X-rays and chromospheric $H\alpha$ emission are thought to be produced by the same magnetic heating mechanisms which are thought to involve either magnetic waves (Goossens 1994) or magnetic reconnection processes (Priest & Forbes 2000) as heating agent. Therefore it is expected to find a correlation between chromospheric and coronal emission when comparing stars at different activity levels. In fact Fleming et al. (1988) and Doyle (1989) have found such a correlation for a sample of dMe flare stars. For the PMS no comparable studies exist mainly because of a lack of $H\alpha$ flux measurements. As we will show in a subsequent paper (Fernández et al., in prep) the non-periodic component of the photometric variability of V410 Tau is reminiscent of flare stars, suggesting that a comparison of its activity to that latter class of objects is justified.

We estimated the X-ray flux of V410 Tau from the ACIS spectrum. The result is given in Table 4. Our optical spectra are not flux-calibrated. But the $H\alpha$ flux can be calculated from $W_{H\alpha}$ with help of the photometry that we can use to determine the continuum flux, because of the very regular pattern of the lightcurve. The $W_{H\alpha}$ was measured on the low-resolution

Table 4. X-ray and $H\alpha$ flux and respective luminosities of V410 Tau during the campaign in November 2001. X-ray emission was measured in the 0.4 – 8 keV energy interval.

<i>Chandra</i>			f_x	$\lg L_x$
Obs-ID			[erg cm ⁻² s ⁻¹]	[erg/s]
200130Q			1.3×10^{-12}	30.5
200190			1.8×10^{-12}	30.6
200191			1.6×10^{-12}	30.5
	$W_{H\alpha}$	R_c	$f_{H\alpha}$	$\lg L_{H\alpha}$
	[Å]	[mag]	[erg cm ⁻² s ⁻¹]	[erg/s]
Min	1.15	10.35	1.9×10^{-13}	29.6
Max	2.45	9.96	5.7×10^{-13}	30.1

spectra, taking into account the photospheric absorption. We multiplied the $W_{H\alpha}$ by the specific flux of the R_c band (in erg s⁻¹cm⁻² Å⁻¹) and used the *Hipparcos* distance for V410 Tau of 136 pc (Wichmann et al. 1998) to compute $L_{H\alpha}$. The specific flux for a star with $R_c = 0$ mag can be obtained from Rydgren et al. (1984), taking into account the central wavelength of the band. We compute the $H\alpha$ flux for the minimum and maximum equivalent width measured in the low-resolution spectra during the quiescence of the star. The corresponding R band brightness is extracted from the lightcurve at the same rotational phase. The minimum and maximum quiescent $H\alpha$ flux during our campaign derived in this way is tabulated in Table 4.

For the M dwarfs studied the X-ray luminosity seems to be somewhat higher than the $H\alpha$ luminosity. Fleming et al. (1988) found the relation $L_{H\alpha} \sim 0.7 L_x$. Similarly, Hawley et al. (1996) quoted values between $\sim 0.2...1$ for $\lg(L_x/L_{H\alpha})$ for both field M dwarfs and the zero-age main sequence cluster IC 2602. The values we derive for the X-ray and $H\alpha$ luminosity of V410 Tau are in good agreement with these relations, suggesting a tight connection between the activity of this PMS star and that of MS flare stars.

7. Conclusion

We have presented the results from a coordinated multi-wavelength observing campaign for the wTTS V410 Tau aiming to disentangle the role that the various atmospheric layers play in magnetic activity. A multi-wavelength approach is essential in establishing the structure and relation between the emission sites.

Our observations of V410 Tau can be summarized as follows:

- An update of the period and ephemeris of the 1.87 d cycle representing the rotation period of the spot dominating since ~ 1990 .
- The non-detection of rotational modulation in the X-ray and $H\alpha$ lightcurves suggests either very long coronal loops or that X-ray emission is not concentrated in the major spot, which extends over the pole of the star but not in a symmetrical way.
- The first tentative detection of an activity cycle on a PMS star seems to indicate that the field generation mechanism

that drives activity in young stars may be more similar to the standard solar-type dynamo than widely believed.

- The detection of flares in both the optical and the X-ray regime, as well as the observed relation between X-ray and H α flux put V410 Tau in close vicinity to the more evolved dMe flare stars.

Whether the characteristics of V410 Tau are peculiar or typical for the PMS, or whether it represents a rare kind of a transition object remains open to date. We would like to encourage systematic multi-wavelength studies of other young stars that will eventually put the nature of magnetic activity on the PMS in a clear context to the case of the Sun and solar-like stars.

Acknowledgements. BS acknowledges financial support from the European Union by the Marie Curie Fellowship Contract No. HPMD-CT-2000-00013. MF is partially supported by the Spanish grant PB97-1438-C02-02. JFG and VC were supported by grant POCTI/1999/FIS/34549 approved by FCT and POCTI, with funds from the European Community program FEDER. We thank the referee W. Herbst for constructive comments. We also want to acknowledge W. Herbst for maintaining the T Tauri photometric database (at <http://www.astro.wesleyan.edu/~bill/>). Finally, we thank P. Amado for careful reading of the manuscript. This research is partly based on data obtained at the 90 cm and 1.5 m telescopes of the Sierra Nevada Observatory (operated by the Consejo Superior de Investigaciones Científicas through the Instituto de Astrofísica de Andalucía), the German-Spanish Astronomical Centre on Calar Alto (operated by the Max-Planck-Institut für Astronomie, Heidelberg jointly with the Spanish National Commission for Astronomy), and the Lick Observatory (operated by the University of California).

References

- Amado P. J., Cutispoto G., Lanza A. F. & Rodonó M., 2001, In: Proc. of the 11th Cambridge Workshop on Cool Stars, Stellar Systems and the Sun, A.S.P. Conf. Proc. 223, R. J. Garcia Lopez, R. Rebolo & M. R. Zapaterio Osorio (eds.), San Francisco: Astronomical Society of the Pacific, 895
- Baliunas S. L., Nesme-Ribes E., Sokoloff D. & Soon W. H., 1996, *ApJ* 460, 848
- Beckwith S., Sargent A., Chini R. S. & Herbst T., 1990, *AJ* 99, 184
- Berdyugina S. V., Pelt J. & Tuominen I., 2002, *A&A* 394, 505
- Bessell M. S., 1983, *PASP* 95, 480
- Bieging J. H. & Cohen M., 1989, *AJ* 98, 1686
- Bieging J. H., Cohen M. & Schwartz P. R., 1984, *ApJ* 282, 699
- Bouvier J. & Bertout C., 1989, *A&A* 211, 99
- Cohen M., Bieging J. H. & Schwartz P. R., 1982, *ApJ* 253, 707
- Collier Cameron A., 2002, *AN* 323, 336
- Costa V. M., Lago M. T. V. T., Norci L. & Meurs E. J. A., 2000, *A&A* 354, 621
- Donati J.-F. & Collier Cameron A., 1997, *MNRAS* 291, 1
- Doyle J. G., 1989, *A&A* 218, 195
- Dworetzky M. M., 1983, *MNRAS* 203, 917
- Fernández M. & Miranda L. F., 1998, *A&A* 332, 629
- Fleming T. A., Liebert J., Gioia I. M. & Maccacaro T., 1988, *ApJ* 331, 958
- Freeman P. E., Kashyap V., Rosner R. & Lamb D. Q., 2002, *ApJS* 138, 185
- Fröhlich H.-E., Tschäpe R., Rüdiger G. & Strassmeier K. G., 2002, *A&A* 391, 659
- Ghez A. M., Neugebauer G. & Matthews K., 1993, *AJ* 106, 2005
- Ghez A. M., White R. J. & Simon M., 1997, *ApJ* 490, 353
- Goossens M., 1994, *Space Science Rev.* 68, 51
- Grankin K. N., 1999, *Astron. Lett.* 25, 8
- Guenther E., Stelzer B., Neuhäuser R., et al., 2000, *A&A* 357, 206
- Gullbring E., Barwig H. & Schmitt J. H. M. M., 1997, *A&A* 324, 155
- Gunn A. G., Mitrou C. K. & Doyle J. G., 1998, *MNRAS* 296, 150
- Hartmann L., Hewett R., Stahler S., & Mathieu R. D., 1986, *ApJ* 309, 275
- Hatzes A. P., 1995, *ApJ* 451, 784
- Hawley S. L., Gizis J. E. & Reid I. N., 1996, *AJ* 112, 2799
- Henry G. W., Eaton J. A., Hamer J. & Hall D. S., 1995, *ApJS* 97, 513
- Herbig G. H. & Bell K. R., 1988, *Lick Obs. Bull.* No 1111, 1 (HBC)
- Herbst W. 1989, *AJ* 98, 2268
- Jardine M., Wood K., Collier Cameron A., Donati J.-F. & Mackay D. H., 2002, *MNRAS* 336, 1364
- Joncour I., Bertout C. & Ménard F., 1994, *A&A* 285, L25
- Kitchatinov L. L., Jardine M. & Collier Cameron A., 2001, *A&A* 374, 250
- Kürster M., Schmitt J. H. M. M., Cutispoto G. & Dennerl K., 1997, *A&A* 320, 831
- Küker M. & Rüdiger G., 1999, *A&A* 346, 922
- Küker M. & Rüdiger G., 1997, *A&A* 328, 253
- Landolt A. U., 1992, *AJ* 104, 340
- Landolt A. U., 1983, *AJ* 88, 853
- Messina S. & Guinan E. F., 2002, *A&A* 393, 225
- Mewe R., Gronenschild E. H. B. M., & van den Oord G. H. J., 1985, *A&AS* 62, 197
- Moss D., Barker D. M., Brandenburg A. & Tuominen I., 1995, *A&A* 294, 155
- Neuhäuser R., Sterzik M. F., Schmitt J. H. M. M., Wichmann R. & Krautter J., 1995, *A&A* 297, 391
- Nielsen R. F., 1983, *Inst.Theor. Astrophys. Oslo Report*, No.59. Ed.O.Hauge, 141
- Nikonov V.B., 1976, *Izv. Krymsk. Astrofiz. Obs.* 54, 3
- Olah K., Kolláth Z. & Strassmeier K. G., 2000, *A&A* 356, 643
- Paresce F. 1984, *AJ* 89, 1022
- Petrov P. P., Shcherbakov V. A., Berdyugina S. V., Shevchenko V. S., Grankin K. N., et al., 1994, *A&AS* 107, 9 (P94)
- Pfeiffer M.J., Frank C., Baumüller D., Fuhrmann K. & Gehren T., 1998, *A&AS*, 130, 381
- Priest E. R. & Forbes T. G., 2000, *Magnetic Reconnection: MHD Theory and Applications* (Cambridge: Cambridge Univ. Press)
- Queloz D., Santos N. C. & Mayor M., 2001, In: Proc. of the First Eddington Workshop on Stellar Structure and Habitable Planet Finding, B. Battrick, F. Favata, I. W. Roxburgh & D. Galadi (eds.), ESA SP-485, Noordwijk: ESA Publications Division, ISBN 92-9092-781-X, 2002, 117

- Rice J. B. & Strassmeier K. G., 1996, A&A 316, 164
- Rodonó M., Messina S., Lanza A. F., Cutispoto G. & Teriaca L., 2000, A&A 358, 624
- Romano G., 1975, Mem. Soc. Astron. Ital. 46, 81
- Rössiger S., 1981, Mitt. Ver. St. 9, 35
- Rydgren A. E. & Vrba F. J., 1983, ApJ 267, 191
- Rydgren A. E., Schmelz J.T., Zak D.S. & Vrba F.J., 1984, Publ. US Naval Obs. XXV, 1
- Sanchez del Rio J. , Ruiz-Falcó Rojas A. & Herpe G., 2000, Rev. Sci. Instruments 71, 2598
- Saar S. H. & Brandenburg A., 1999, ApJ 524, 295
- Saar S. H. & Donahue R. A., 1997, ApJ 485, 319
- Shevchenko V.S., 1980, Astron. Zh., 57, 1162
- Snodgrass H. B., 1983, ApJ 270, 288
- Stelzer B., Fernández M., Costa V., Grankin K., Henden A., et al., 2002, In: Sunspots & Starspots, 1st Potsdam Thinkshop, K. Strassmeier (ed.), Brandenburgische Universitätsdruckerei, Golm, Germany
- Stelzer B. & Neuhäuser R., 2001, A&A 377, 538
- Strassmeier, K. G., Bartus, J., Cutispoto, G. & Rodonó, M., 1997 A&AS 125, 11
- Strassmeier, K. G., Welty, A. D. & Rice, J. B., 1994, A&A 285, L17
- Strom K. M. & Strom S. E., 1994, ApJ 424, 237
- Tonry J. & Davis M., 1979, AJ 84, 1511
- Ventura P., Zeppieri A., Mazzitelli I. & D'Antona F., 1998, A&A 331, 1011
- Vogel S. N. & Kuhi L. V., 1981, ApJ 245, 960
- Vogt S. S. & Penrod G. D., 1983, PASP 95, 565
- Vogt S. S., Penrod G. D. & Hatzes A. P., 1987, ApJ 321, 496
- Vrba F. J., Herbst W. & Booth J. F., 1988, AJ 96, 1032
- Wallace L., Livingston W., Hinkle K. & Bernath P., 1996, ApJS 106, 165
- Welty A. D. & Ramsey L. W., 1995, AJ 110, 336
- Wichmann R., Bastian U., Krautter J., Jankovics I. & Rucinski S. M., 1998, MNRAS 301, L39